R4496C RyR2 mutation impairs atrial and ventricular contractility

Cecilia Ferrantini,[1] Raffaele Coppini,[1] Beatrice Scellini,[1] Claudia Ferrara,[1] Josè Manuel Pioner,[1] Luca Mazzoni,[1] Silvia Priori,[2] Elisabetta Cerbai,[1] Chiara Tesi,[1] and Corrado Poggesi[1]

[1]Center for Molecular Medicine and Applied Biophysics, University of Florence, 50121 Florence, Italy
[2]IRCCS Fondazione Salvatore Maugeri, 27100 Pavia, Italy

Ryanodine receptor (RyR2) is the major Ca^{2+} channel of the cardiac sarcoplasmic reticulum (SR) and plays a crucial role in the generation of myocardial force. Changes in RyR2 gating properties and resulting increases in its open probability (P_o) are associated with Ca^{2+} leakage from the SR and arrhythmias; however, the effects of RyR2 dysfunction on myocardial contractility are unknown. Here, we investigated the possibility that a RyR2 mutation associated with catecholaminergic polymorphic ventricular tachycardia, R4496C, affects the contractile function of atrial and ventricular myocardium. We measured isometric twitch tension in left ventricular and atrial trabeculae from wild-type mice and heterozygous transgenic mice carrying the R4496C RyR2 mutation and found that twitch force was comparable under baseline conditions (30°C, 2 mM $[Ca^{2+}]_o$, 1 Hz). However, the positive inotropic responses to high stimulation frequency, 0.1 µM isoproterenol, and 5 mM $[Ca^{2+}]_o$ were decreased in R4496C trabeculae, as was post-rest potentiation. We investigated the mechanisms underlying inotropic insufficiency in R4496C muscles in single ventricular myocytes. Under baseline conditions, the amplitude of the Ca^{2+} transient was normal, despite the reduced SR Ca^{2+} content. Under inotropic challenge, however, R4496C myocytes were unable to boost the amplitude of Ca^{2+} transients because they are incapable of properly increasing the amount of Ca^{2+} stored in the SR because of a larger SR Ca^{2+} leakage. Recovery of force in response to premature stimuli was faster in R4496C myocardium, despite the unchanged rates of recovery of L-type Ca^{2+} channel current (I_{Ca-L}) and SR Ca^{2+} content in single myocytes. A faster recovery from inactivation of the mutant R4496C channels could explain this behavior. In conclusion, changes in RyR2 channel gating associated with the R4496C mutation could be directly responsible for the alterations in both ventricular and atrial contractility. The increased RyR2 P_o and fractional Ca^{2+} release from the SR induced by the R4496C mutation preserves baseline contractility despite a slight decrease in SR Ca^{2+} content, but cannot compensate for the inability to increase SR Ca^{2+} content during inotropic challenge.

INTRODUCTION

The cardiac RyR2 is the main SR Ca^{2+} release channel (Franzini-Armstrong and Protasi, 1997; Bers and Fill, 1998; Lanner et al., 2010). Large amounts of SR Ca^{2+} are released into the cytosol through RyR2 in response to small localized elevations of cytosolic $[Ca^{2+}]$, generated by Ca^{2+} entry through L-type Ca^{2+} channels during action potentials (CICR). The SR, via RyR2, releases 70–90% of the total Ca^{2+} that activates contraction (Bers, 2002). The amplitude of Ca^{2+} transients depends directly on SR Ca^{2+} content (Bers, 2002) and RyR2 channel gating properties. Importantly for normal Ca^{2+} cycling, the SR becomes refractory after each systolic Ca^{2+} release, preventing spontaneous reactivation of CICR during the diastolic period (Brunello et al., 2013). RyR2 channel refractoriness plays a major role in this regulation (Kornyeyev et al., 2012; Brunello et al., 2013).

RyR2 genetic mutations or acquired defects (e.g., increased phosphorylation of the channel in heart failure) are well known to predispose individuals to arrhythmias (George et al., 2007). However, their impact on contractile function is considered of minor clinical relevance and has been poorly investigated. Mutations in the RyR2 gene were the first to be associated with catecholaminergic polymorphic ventricular tachycardia (CPVT) (Laitinen et al., 2001), and the single amino acid substitution R4497C is one of the earliest RyR2 mutations identified in CPVT patients (Priori et al., 2002). CPVT is characterized by stress-induced syncopal episodes underlying events of ventricular tachycardia (Priori et al., 2002) with a cumulative risk of sudden death of 30–50% by age 35. No echocardiographic signs of contractile impairment are usually found in young CPVT patients, but aging or concurrent acquired disease (Kannankeril et al., 2006) may more easily promote contractile dysfunction.

Experiments on single channels or channels reexpressed in cellular vectors (Jiang et al., 2002) showed that many of the CPVT-associated mutant RyR2 (including R4497C) channels exhibit an increased sensitivity to

---

C. Ferrantini and R. Coppini contributed equally to this paper.
Correspondence to Cecilia Ferrantini: cecilia.ferrantini@unifi.it

Abbreviations used in this paper: CPVT, catecholaminergic polymorphic ventricular tachycardia; DAD, delayed afterdepolarization; NCX, Na^{2+}–Ca^{2+} exchanger; P_o, open probability.

The Journal of General Physiology

cytosolic and/or SR luminal Ca^{2+} ($[Ca^{2+}]_{SR}$), and thus an increased open probability (P_o) and a lower threshold for SR Ca^{2+} overspill. Consistently, in the myocardium of RyR2 mutation carriers, increase in SR Ca^{2+} content by inotropic stimuli (e.g., β-adrenergic stimulation, ouabain) enhances aberrant diastolic SR Ca^{2+} release initiating calcium waves (Sedej et al., 2010) and delayed afterdepolarizations (DADs) (Mohamed et al., 2007; Chen et al., 2012).

Besides promoting cellular arrhythmias (Kashimura et al., 2010), SR Ca^{2+} leakage during diastole may reduce the amount of SR Ca^{2+} available for systolic release and myofilament activation. To investigate whether RyR2 mutations alter systolic Ca^{2+} release and contractile function, we used trabeculae and myocytes from transgenic mice carrying the R4496C RyR2 mutation (Cerrone et al., 2005) (equivalent to R4497C human mutation). R4496C mice show a clear arrhythmogenic phenotype under β-adrenergic stimulation (Liu et al., 2006), resembling the human disease. Here we aim to study whether a RyR2 mutation associated with CPVT affects atrial and ventricular contractile function. In brief, we found that atrial and ventricular myocardium from R4496C mice show impaired force responses to positive inotropic stimuli, related to blunted SR Ca^{2+} load potentiation and increased SR Ca^{2+} leakage. The altered gating properties of the RyR2 channel caused by the single amino acid substitution appear to be the sole determinants of the observed abnormalities. Collectively, our results suggest that disease-related primary or secondary modifications of the RyR2, leading to increased P_o of the channel, not only cause arrhythmias but also determine contractile impairment in the heart.

MATERIALS AND METHODS

Animal model
We used a knock-in mouse model of CPVT carrying the R4496C RyR2 gene mutation (Cerrone et al., 2005). Suitable trabeculae for mechanical experiments are found more frequently in 129SV/J than in C57BL/6 hearts. Therefore, heterozygous transgenic progenitors with a C57BL/6 genetic background were bred to 129SV/J mice (Charles River) to obtain crossbred mutant carriers. First-generation heterozygous crossbred mice were bred to WT 129SV/J for four generations to obtain mutant carriers bearing a 129SV/J-like phenotype.

The genotypes from the crossbred generations were determined by PCR on DNA from tail biopsy specimens. Persistence of CPVT phenotype in our crossbred strain was confirmed by electrophysiological measurements in isolated myocytes. Animals used for experiments were 16–20-wk-old males weighing 25–35 g. Animals were maintained and bred at the animal facility of the University of Florence. Animals were bred and used for experiments in accordance with Italian and European regulations for animal handling and care, and all experimental protocols were approved by the local committee for animal welfare.

Intact cardiac preparations
Right ventricular and left atrial trabeculae were isolated from mouse hearts as described previously (Stull et al., 2002). In brief,

male WT ($n = 20$) or heterozygous R4496C mutant ($n = 22$) mice were heparinized and anesthetized by inhaled isoflurane. Hearts were rapidly excised and perfused retrogradely with a Krebs–Henseleit buffer containing (mmol/L): 120 NaCl, 5 KCl, 2 $MgSO_4$, 1.2 NaH_2PO_4, 20 $NaHCO_3$, 1.8 $CaCl_2$, and 10 glucose, pH 7.4 with 95% O_2/5% CO_2. 20 mM BDM (2,3-butanedione-monoxime) was added to the dissection buffer to reduce cutting injury. The right ventricle was opened by cutting along the anterior interventricular junction. Thin unbranched trabeculae, running between the free wall of the right ventricle and the atrioventricular ring, were dissected by cutting through the atrioventricular ring on one extremity and removing a portion of the right ventricular wall on the other one. The left atrial appendage was gently separated from the remaining cardiac tissue and cut open. Free-running atrial trabeculae were dissected, leaving a block of tissue at both ends to facilitate mounting. Cross-sectional muscle area was calculated with the assumption of an ellipsoid shape.

Isolation of ventricular cardiomyocytes from mouse hearts
Left ventricular cells were isolated from male adult WT ($n = 16$) or heterozygous R4496C mutant ($n = 18$) mice as described previously (Shioya, 2007). In brief, excised hearts were immediately bathed in HEPES buffer (HB) and cannulated through the aorta for retrograde perfusion at a constant flow of 3 ml/min. The HB contained (mM): 132 NaCl, 4 KCI, 1.2 $MgCl_2$, 10 HEPES, and 10 glucose, pH 7.35 with NaOH. We then added 0.1 mg/ml Liberase TM (Roche) to the HB, and this enzyme solution was recirculated for 7–8 min. From the digested heart, the left ventricle was excised and shredded into several pieces with gentle stirring. The cell suspension was centrifuged, and the cell pellet ($\sim$0.1 ml) was resuspended in standard Tyrode's buffer (see below) supplemented with 0.1 mM $CaCl_2$ and 1 mg/ml BSA. Ca^{2+} concentration was gradually raised up to 1 mM, and isolated cells were stored at room temperature (20°C).

Mechanical measurements on intact trabeculae
Ventricular and atrial trabeculae were mounted between the basket-shaped platinum end of a force transducer (KG7A; Scientific Instruments-Heidelberg) and a motor (Aurora Scientific Inc.), both connected to micromanipulators, in a glass-bottomed heated horizontal tissue bath with platinum wires for field stimulation. Sarcomere length was measured by laser diffraction (Ferrantini et al., 2014). Custom-made software (LabVIEW) was used for motor control, stimulation, and force signal recording.

Muscles were allowed to stabilize at baseline conditions (30°C, 2 mmol/L [$CaCl_2$], 1 Hz stimulation) for at least 20–30 min and were gradually stretched to optimal initial sarcomere length (2.15 ± 0.03 μm) before starting the experimental protocol.

Twitch force and kinetics were studied with the following protocols.

Response to varied extracellular [Ca^{2+}] or isoproterenol. Twitch force was measured at 1 Hz, with [Ca^{2+}]$_{out}$ varying between 1 and 10 mM. Muscles were exposed to a saturating dose of isoproterenol (1 μM); recordings were started 10 min after each solution change.

Force–frequency relationship. Trabeculae were paced at different stimulation frequencies (0.1–8 Hz) to assess changes of steady-state twitch force.

Post-rest potentiation. Stimulation pauses of different duration (2–60 s) were inserted after the last contraction of a steady series at 1 Hz to evaluate post-rest potentiation of the first stimulated beat after the pause.

Mechanical restitution and post-extrasystolic potentiation. After 30 s of stimulation at 1 Hz, a premature stimulus was given at

different premature intervals (from 50 to 900 ms), determining a premature contraction (extrasystole) that was reduced in amplitude. The relative amplitudes of premature beats were plotted against the corresponding stimulus intervals, and the restitution curve was fitted using a single exponential to calculate the restitution rate. Stimulation was resumed 1 s after the premature beat, and the force of the first subsequent beat was measured to evaluate post-extrasystolic potentiation.

Electrophysiological and intracellular Ca^{2+} measurements in intact cardiomyocytes

Freshly isolated cardiomyocytes were used for action potentials, ionic currents, and intracellular Ca^{2+} measurements. Action potentials or ionic currents were measured under current- and voltage-clamp conditions, respectively, using either the whole-cell perforated-patch or ruptured-patch configurations of the patch-clamp technique. Myocytes were loaded with Ca^{2+} indicator by a 30-min incubation with 10 µmol/L Fluoforte (Enzo Life Sciences). Cell suspension was then transferred to a temperature-controlled recording chamber with a continuous flow rate of 0.3 ml/min (30 ± 0.5°C), mounted on the stage of an inverted microscope. A rapid solution–change system (Warner Instruments) with a multi-barreled pipette allowed fast (<3-ms) exchange of the solution bathing the cell under study.

For perforated-patch experiments, we used the amphotericin method. For action potential recordings, the pipette solution contained (mM): 115 potassium methanesulfonate, 25 KCl, 10 HEPES, and 3 $MgCl_2$. The standard Tyrode's buffer contained (mM): 136 NaCl, 5.4 KCl, 0.33 Na_2PO_4, 1.8 $CaCl_2$, 1 $MgCl_2$, 10 dextrose, and 10 HEPES-NaOH, pH 7.35 (NaOH). For calcium current (I_{Ca-L}) recordings, the pipette contained (mM): 80 cesium methanesulfonate, 40 CsCl, 10 HEPES, 1 KCl, and 1 $CaCl_2$, pH 7.4 (CsOH). The bathing solution contained (mmol/L): 140 NaCl, 6 CsCl, 10 glucose, 10 HEPES, 1 $MgCl_2$, 2 $CaCl_2$, 0.02 niflumic acid, and 0.02 TTX, pH 7.4 (CsOH). Ruptured-patch experiments were used to record SR calcium content. The pipette solution contained (mM): 110 K^+-aspartate, 23 KCl, 0.4 $CaCl_2$ (calculated free $Ca^{2+} = 10^{-7}$ M), 3 $MgCl_2$, 5 HEPES-KOH, 1 EGTA-KOH, 0.4 GTP-Na^+, 5 ATP-Na^+, and 5 creatine phosphate, pH 7.3 (KOH). Potential and current signals were measured with an amplifier (700B Multiclamp) and digitized through an A/D converter (Digidata 1440A), using dedicated software (pClamp 10; all from Molecular Devices).

Intracellular Ca^{2+} measurements were simultaneously performed on patched cells. Fluoforte fluorescence emitted at 513 nm was measured during fixed excitation at a 492-nm wavelength. At the end of the recording protocol, each cell was mechanically permeabilized to record the maximal fluorescence used for signal normalization.

The following protocols were used in single cells.

Current-clamp protocols. Action potentials/Ca^{2+} transients were elicited with small depolarizing stimuli. Steady-state action potential/calcium transients were evaluated upon stimulation at 1–4 Hz at steady state (>1 min). Post-rest action potential/Ca^{2+} transients were studied by stimulating the cell at 3 Hz for 20 s before interrupting pacing for a variable resting interval, from 500 ms to 20 s. Calcium transient restitution was evaluated by stimulating the cell at 1 Hz for 15 s before introducing a premature stimulus at a variable interval, from 50 to 900 ms: relative Ca^{2+}-transient amplitude at each premature interval was plotted against interval duration to obtain a restitution curve. To assess membrane refractoriness, the myocyte was paced at a cycle length of 1,000 ms for 10 beats, and then an extrastimulus (S2) was delivered at progressively shorter S1S2 coupling intervals (in 5-ms increments) until loss of capture. The rate of DADs was evaluated during stimulation pauses after a 3-Hz conditioning stimulation in the presence of isoproterenol (30 nmol/L). DADs were scored when spontaneous intracellular Ca^{2+} oscillations generated a >20-mV membrane depolarization.

Voltage-clamp protocols. I_{Ca-L} current–voltage relationship was recorded by imposing 200-ms depolarizing steps from −50 to 50 mV from a holding potential of −80 mV. I_{Ca-L} restitution was evaluated by inserting a premature 50-ms depolarizing step to 0 mV after 15 conditioning depolarizing steps at 1 Hz, at variable intervals ranging from 30 to 950 ms. Finally, SR Ca^{2+} content was studied as follows: after 30–50-ms conditioning steps to 0 mV at 1 Hz (holding = 80 mV) in normal Tyrode's solution, bathing solution was rapidly switched to expose the cell to 10 mmol/L caffeine for 10 s. Inward Na^{2+}–Ca^{2+} exchanger (NCX)-mediated current during the 10 s of caffeine exposure was integrated to calculate the total amount of charge crossing the membrane (C_{caff}). Total SR Ca^{2+} content (expressed as millimole per liter of cytosol) was calculated as follows: $[Ca^{2+}]_{SR} = [(1 + 0.12)(C_{caff}/F \times 1,000)]/(Cm*8.31)$, where Cm = membrane capacitance and F = Faraday's number (96,500 C/M). The same process was repeated using 2- or 3-Hz conditioning steps (see also Fig. 6). Timing of caffeine exposure was adjusted to get premature or longer intervals from the last conditioning steps: 100–900-ms premature intervals and 2–8-s resting intervals were tested to, respectively, assess SR Ca^{2+} content recovery and SR Ca^{2+} accumulation during pauses. Baseline frequency was 1 Hz for the recovery protocol and 3 Hz for the pauses protocol. The recovery of SR Ca^{2+} content was also analyzed by quantifying the relative amplitude of premature caffeine-induced Ca^{2+} transients with respect to the caffeine-transient evoked 1 s after the last paced beat. At earlier intervals (100–300 ms), the onset of caffeine transient occurred before the end of the last regular transient; therefore, the shape of the average of 10 regular 1-Hz transients (recorded during the conditioning train of stimuli) was subtracted from the fused trace (see Fig. 8 for details).

Statistical analysis

Data are expressed and plotted as the mean ± SEM obtained from several independent determinations on different myocytes or trabeculae. Number of cells/trabeculae (n) and number of animals (N) are indicated in the figure legends for each set of measurements. Unpaired Student's t test is used for comparisons. A p-value of <0.05 is considered statistically significant. All measurements aimed at comparing WT to R4496C preparations are based on the following assumptions: (a) the variance of different preparations derived from single animals is comparable with the variance found among different animals, and (b) the number of preparations derived from each animal is comparable.

Mathematical modeling

Using the COR CellML platform (Garny et al., 2009), we developed a comprehensive mathematical model of WT and R4496C ventricular cardiomyocytes. A RyR2 gating function featuring channel modulation by cytosolic and luminal $[Ca^{2+}]$ (Iyer et al., 2007) was inserted into a cardiomyocyte model, derived from Shannon et al. (2004), adapted to the mouse (Bondarenko et al., 2004), and included a function of isometric force generation (Rice et al., 1999). Changes of RyR2 gating caused by R4496C mutation were simulated in the model through appropriate adjustments of RyR2 gating parameters to fit previous data from single mutant RyR2 channels (Jiang et al., 2002) and our experimental results. The model could emulate the experimental protocols performed in cells and trabeculae.

Online supplemental material

The online supplement includes a detailed description of the mathematical model, including an account of the kinetic model of RyR2 gating (Fig. S1) and of the composition of the mouse

cardiomyocyte model, an overview of the experiments performed to validate the model, as well as an explanation on how the constants describing the behavior of mutant modeled cardiomyocytes were derived (Fig. S2). The ability of the model to predict experimental results is shown in Fig. S3. The complete model file comprising the full set of equations can be found as an online supplement (R4496C_model.cellml) and can be run using freely available CellML programs such as COR or OpenCell (http://cellml.org/tools/modeling-environments). The online supplemental material is available at http://www.jgp.org/cgi/content/full/jgp.201511450/DC1.

RESULTS

Blunted inotropic responses in R4496C myocardium

Under basal experimental conditions (30°C, 1-Hz stimulation rate, 2 mM $[Ca^{2+}]_{out}$), no changes in isometric twitch tension and kinetics were found between R4496C and WT atrial and ventricular trabeculae (Table 1). Notably, atrial trabeculae display lower tension and faster twitch kinetics when compared with corresponding ventricular trabeculae, in line with previous comparisons of atrial and ventricular myocardium from different mammalian species (Ásgrímsson et al., 1995).

Differences in peak twitch tension between R4496C and WT trabeculae became evident after inotropic stimulation of atrial and ventricular myocardium. Peak tension was lower in R4496C than in WT preparations in response to interventions aimed to markedly increase isometric twitch force, i.e., 10^{-7} M isoproterenol (Iso) and 5 mM $[Ca^{2+}]_{out}$ (Fig. 1 and Table 1). Despite these blunted positive inotropic responses, changes in contraction kinetics caused by the inotropic interventions were still present and comparable to those found in WT trabeculae. In particular, Iso accelerated twitch force generation and relaxation, whereas the application of 5 mM $[Ca^{2+}]_{out}$ determined a slight prolongation of twitch
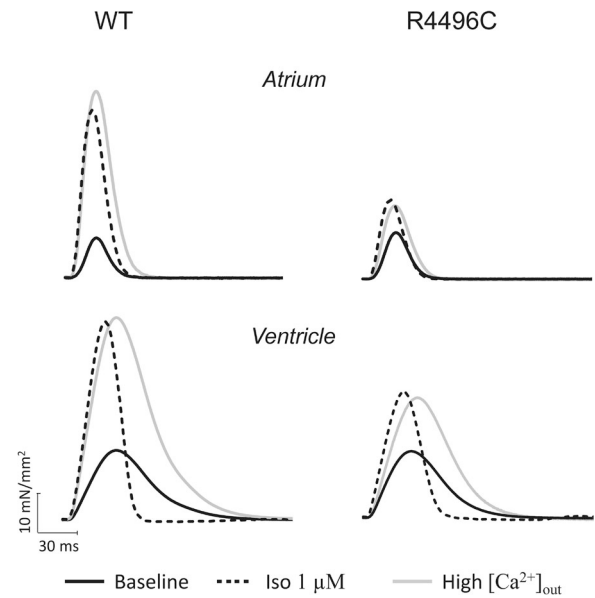
Figure 1. Response to isoproterenol and high $[Ca^{2+}]_{out}$. Representative traces from atrial (top) and ventricular (bottom) WT (left) and R4496C (right) trabeculae at baseline (1 Hz, 2 mM $[Ca^{2+}]_{out}$, 30°C; black traces), under isoproterenol (10 µM; light gray traces), and in high extracellular calcium (8 mM $[Ca^{2+}]_e$; dark gray traces). For average values see Table 1.

duration in both WT and R4496C ventricular preparations (Fig. 1 and Table 1). Notably, negligible changes of contraction kinetics in response to Iso or 5 mM $[Ca^{2+}]_{out}$ were observed in atrial trabeculae from both WT and R4496C mice.

Despite a similar twitch amplitude at 1 Hz, when stimulation frequency was increased to 5 Hz, the physiological rate-dependent increase of contractile force was significantly blunted in R4496C atrial and ventricular preparations as compared with WT trabeculae (Fig. 2 A).

TABLE 1

Isometric twitch-tension parameters at basal conditions (30°C, 2 mM $[Ca^{2+}]_{out}$, 1-Hz stimulation rate) and in the presence of 10^{-6} M isoproterenol or high extracellular calcium (8 mM $[Ca^{2+}]_{out}$).

Parameter	Atrial trabeculae			Ventricular trabeculae		
	WT (n = 12)	R4496C (n = 10)	P value	WT (n = 12)	R4496C (n = 11)	P value
Basal conditions						
Peak tension (mN/mm²)	11.3 ± 1.3	12.9 ± 2.4	NS	26.0 ± 4.4	26.8 ± 4.5	NS
Time to peak (ms)	44.9 ± 2.4	44.7 ± 1.7	NS	63.4 ± 4.2	64.9 ± 3.7	NS
Time to 50% relaxation (ms)	24.1 ± 1.1	24.8 ± 2.2	NS	42.3 ± 1.7	46.1 ± 1.8	NS
Isoproterenol						
Peak tension (mN/mm²)	49.3 ± 8.3	22.9 ± 6.4	<0.01	66.3 ± 12.4	41.8 ± 8.5	<0.05
Time to peak (ms)	39.3 ± 4.4	37.7 ± 3.7	NS	43.7 ± 3.6	44.9 ± 3.7	NS
Time to 50% relaxation (ms)	17.5 ± 2.1	18.1 ± 2.2	NS	22.3 ± 1.9	23.1 ± 1.8	NS
High extracellular calcium						
Peak tension (mN/mm²)	47.2 ± 8.6	25.2 ± 5.6	<0.05	65.4 ± 12.2	49.1 ± 9.0	<0.05
Time to peak (ms)	47.6 ± 3.3	48.4 ± 2.6	NS	64.1 ± 3.6	64.5 ± 4.1	NS
Time to 50% relaxation (ms)	25.8 ± 2.7	27.1 ± 3.1	NS	45.3 ± 4.8	46.5 ± 2.3	NS

Values are expressed as means ± SEM. The p-value is estimated by the Student's t test. The number in parentheses is the number of preparations. Time to peak is the time from stimulus to peak contraction. Time to 50% relaxation is the time from peak to 50% decay of force.

In spite of some different reports in isolated myocytes (Fernández-Velasco et al., 2009), the relation between tension and stimulation frequency is biphasic in intact mouse myocardium, with a descending limb (0.1–1 Hz at 30°C) and an ascending limb (1–10 Hz) (Stull et al., 2002; Stuyvers et al., 2002). The slope of the ascending limb of the force–frequency relationship was depressed in R4496C atrial and ventricular trabeculae compared with WT preparations (Fig. 2 B). Rate adaptation of twitch duration (i.e., acceleration of contraction kinetics with increase in stimulation frequency) was preserved in R4496C ventricular myocardium (Fig. 2 B). Interestingly, both WT and R4496C atrial trabeculae show no or minimal rate adaptation of twitch duration.

When a stimulation pause was applied during a series of regularly paced twitches at 1 Hz, the increase in amplitude of the first twitch after the pause was significantly blunted in R4496C preparations compared with WT (Fig. 3 A). In all preparations, post-rest potentiation of twitch tension depended on the duration of the rest pause (Fig. 3 B). Maximum post-rest potentiation was markedly lower in R4496C than in WT atrial and ventricular trabeculae and was reached at shorter rest intervals. Accordingly, steady-state twitches elicited at

low pacing frequencies (0.1–0.5 Hz) were blunted in R4469C myocardium (Fig. 2 B). These results confirm the decreased ability of R4496C myocardium to increase force in response to positive inotropic interventions. Of note, in WT myocardium, all positive inotropic interventions (isoproterenol, pauses, high frequency) lead to a larger fractional increase of force in the atria, suggesting a higher inotropic reserve in atrial versus ventricular myocardium, as described previously (Ásgrímsson et al., 1995).

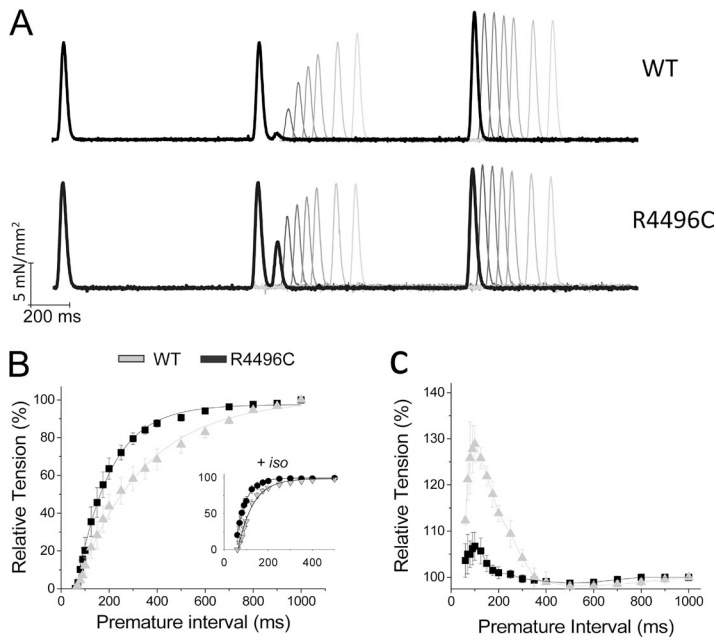### Faster mechanical restitution in R4496C myocardium

Mechanical restitution was studied by introducing a premature stimulus into a regular stimulus sequence: the associated contraction (extrasystole) was reduced in amplitude (Fig. 4 A). The force of the extrasystolic beat increases with increasing the interval preceding the premature stimulus, until the steady-state force is again established (mechanical restitution) (Cooper and Fry, 1990). Mechanical restitution curves display the fractional recovery of force (premature twitch force/steady-state twitch force) plotted against the premature stimulus interval. Mechanical restitution was faster in R4496C
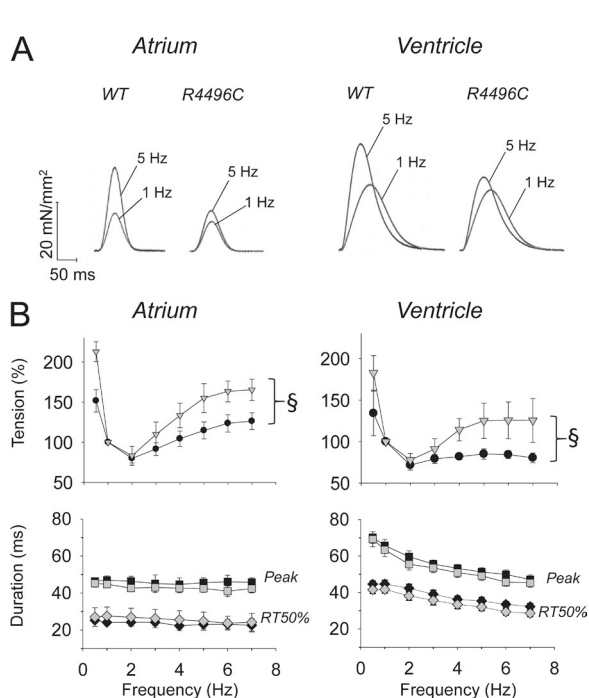
Figure 2. Steady-state force–frequency relationship. Representative traces (A) and mean (±SE) twitch tension (B; top) show a flattened force–frequency relationship in R4496C atrial and ventricular trabeculae when compared with WT preparations. Tension is normalized to 1-Hz twitch amplitude. § = P < 0.05 for 4–7-Hz frequencies. In atrial preparations, relative force at 0.5 Hz was also significantly lower in R4496C versus WT trabeculae. (Bottom) No differences were found in the kinetics of twitches at different frequencies of stimulation (Peak, time to peak contraction; RT50, time to 50% relaxation). Error bars represent mean ± SEM.
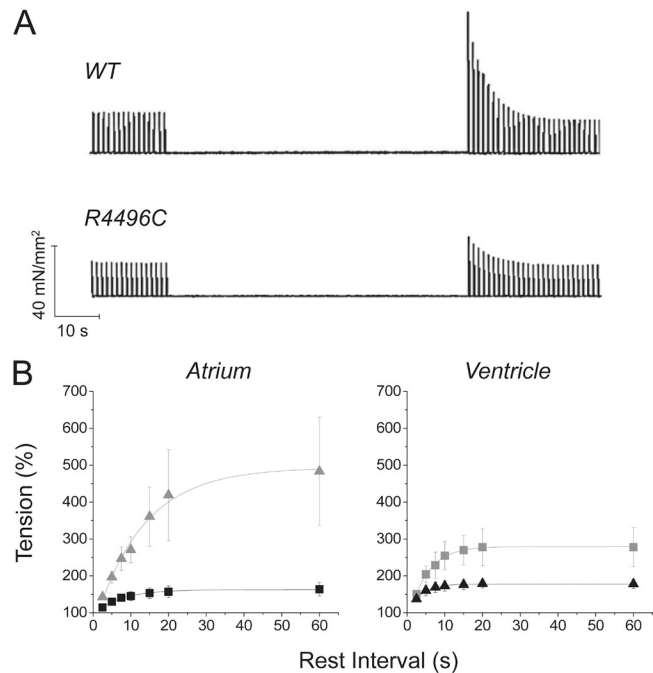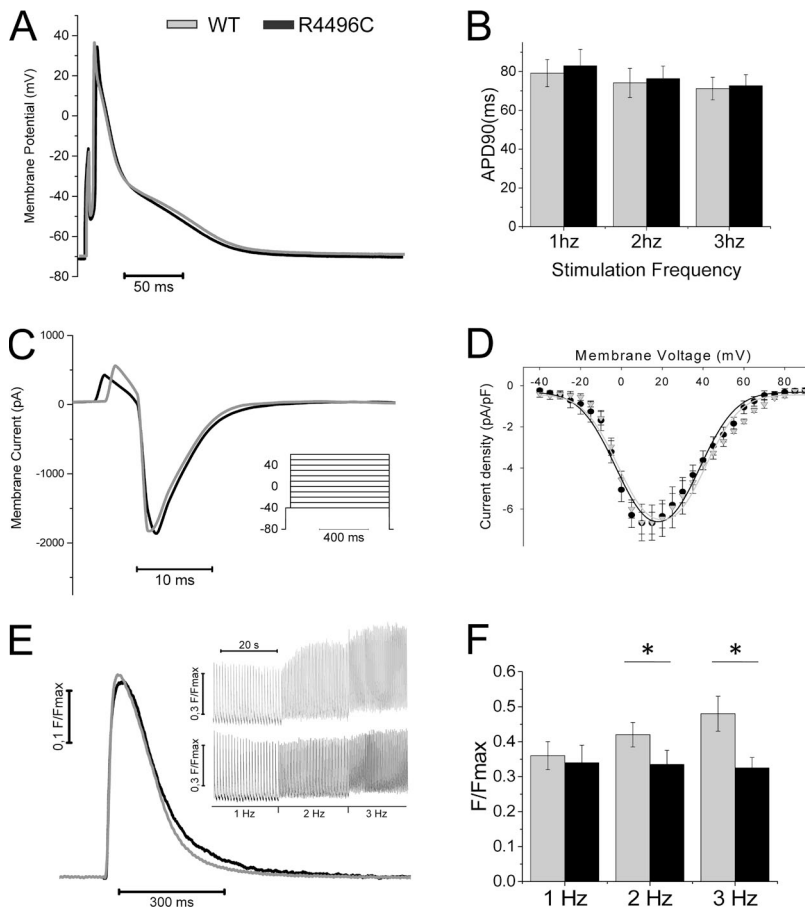
Figure 3. Post-rest potentiation. (A) Traces showing reduced maximal post-rest force in a typical R4496C ventricular trabecula compared with WT. (B) Average percent increase of twitch force after different intervals of stimulation pauses from a basal frequency of 1 Hz in atrial (left) and ventricular (right) R4496C versus WT trabeculae. In atrial trabeculae, absolute maximal post-rest twitch force at a 60-s rest interval was 53.3 ± 9.6 mN/mm² in WT versus 19.9 ± 4.6 mN/mm² in R4496C (P < 0.01). In ventricular trabeculae, maximal post-rest twitch force at a 60-s rest interval was 76.3 ± 15.6 mN/mm² in WT versus 44.3 ± 8.6 mN/mm² in R4496C (P < 0.01). Error bars represent mean ± SEM.

A

WT

R4496C

5 mN/mm²
200 ms

B

WT ▢   R4496C ■

Relative Tension (%)

+ iso

Premature interval (ms)

C

Relative Tension (%)

Premature Interval (ms)

Figure 4. Mechanical restitution in atrial trabeculae. Restitution curves show the fractional recovery (percentage of 1 Hz steady-state peak value) of force in response to the premature stimulus plotted against the premature interval. Each curve was fitted by a single exponential to obtain restitution rates ($1/\tau$): average rates are indicated below. (A) Restitution protocol: representative traces from a WT atrial trabecula (above) and a R4496C atrial muscle (below). The subsequent trials with increasing premature interval of the extra beat are shown superimposed in different colors (black to light gray). (B) Average restitution curves from WT (gray) and R4496C (black) atrial trabeculae. Rates: 5.0 ± 0.9 s^{-1} in WT and 9.0 ± 0.9 s^{-1} in R4496C; $P < 0.05$. (Inset) Restitution curves from WT and R4496C atrial trabeculae upon superfusion with 5×10^{-7} mol/L isoproterenol. Rates: 14.6 ± 1.1 s^{-1} in WT and 25.5 ± 4.7 s^{-1} in R4496C; $P < 0.05$. (C) Post-extrasystolic potentiation. The graph displays the relative tension of the first beat after the extrasystole plotted against the premature interval. Potentiation is significantly less pronounced in R4496C atrial trabeculae ($P < 0.05$ for intervals between 50 and 250 ms). Error bars represent mean ± SEM.

versus WT trabeculae from both atrial and ventricular muscle (Fig. 4, A and B; see Fig. 8 A for ventricular trabeculae). Notably, force recovery was always faster in atrial than in ventricular muscles, likely reflecting faster SR Ca^{2+} uptake rate in the atria (Korajoki and Vornanen, 2012).

β-Adrenergic stimulation, by maximally speeding up SR Ca^{2+} uptake, accelerated mechanical restitution in both WT and R4496C preparations (Fig. 4 B, inset). However, recovery of isometric force in the presence of isoproterenol was still significantly faster in R4496C trabeculae as compared with WT muscles. Notably,

A

WT ▢   R4496C ■

Membrane Potential (mV)

50 ms

B

APD90(ms)

1hz   2hz   3hz
Stimulation Frequency

C

Membrane Current (pA)

10 ms

400 ms

D

Membrane Voltage (mV)

Current density (pA/pF)

E

0.1 F/Fmax

0.3 F/Fmax

0.3 F/Fmax

20 s

1 Hz   2 Hz   3 Hz

300 ms

F

F/Fmax

*   *

1 Hz   2 Hz   3 Hz

Figure 5. Action potentials, L-type Ca^{2+} current, and intracellular Ca^{2+} transients in R4496C myocytes. (A) Representative superimposed action potentials evoked at 1 Hz in WT ($n = 28$ and 9) and R4496C ($n = 30$ and 10) myocytes. (B) Average action potential duration at 90% repolarization (APD90) at 1-, 2-, and 3-Hz pacing rates. (C) Representative superimposed L-type Ca^{2+} current (I_{CaL}) traces from WT and R4496C cardiomyocytes evoked with a 1.5-s depolarization at 5 mV. (Inset) Patch-clamp protocol for I_{CaL} current–voltage relationship. (D) Average I_{CaL} current–voltage relationship curves in WT ($n = 28$ and 9) and R4496C ($n = 30$ and 10) ventricular myocytes. (E) Superimposed representative Ca^{2+}-transient recording under current clamp while stimulating at 1 Hz in WT and R4496C myocytes. (Inset) Representative traces of Ca^{2+} transients from current-clamped R4496C (below) and WT (above) ventricular myocytes at different frequencies of stimulation. (F) Average amplitude of Ca^{2+} transients at 1-, 2-, and 3-Hz pacing rates in WT ($n = 17$ and 7) and R4496C ($n = 18$ and 8) myocytes. *, $P < 0.01$ versus WT; unpaired Student's t test. Error bars represent mean ± SEM.

post-extrasystolic potentiation was reduced in R4496C versus WT atrial trabeculae (Fig. 4 C), in line with the observed reduction of post-rest potentiation in R4496C myocardium.

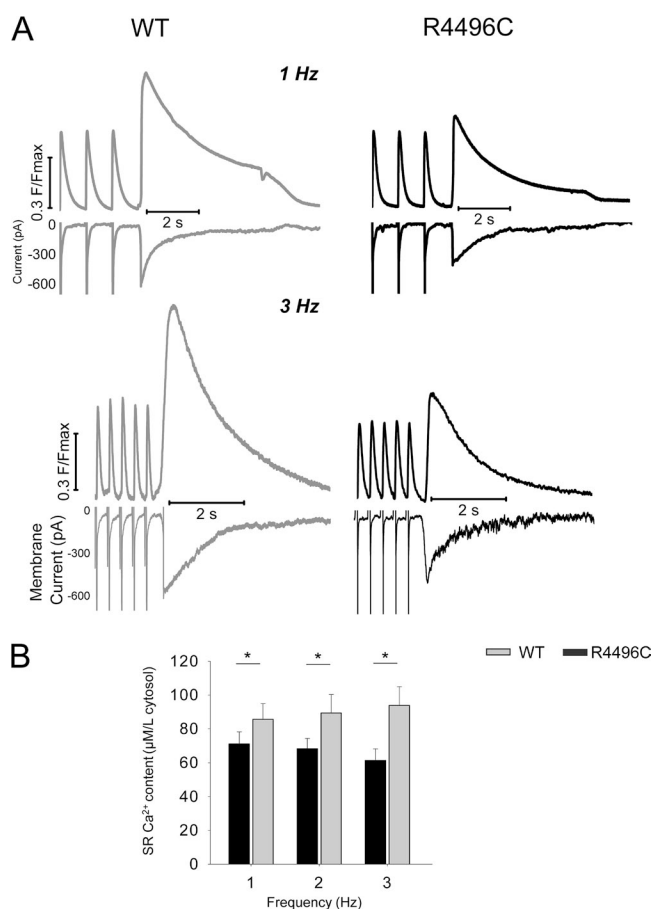### Mechanisms underlying the blunted inotropic response of R4496C myocardium

To better understand the mechanisms underlying the blunted inotropic response of R4496C trabeculae, we investigated excitation–contraction coupling of single ventricular cardiomyocytes from R4496C and WT hearts by simultaneous patch clamp and intracellular Ca^{2+} measurements. Patch-clamp experiments showed that no significant alterations of basal membrane electrical activity were present in R4496C ventricular myocytes. Duration of action potentials was comparable at all frequencies investigated in WT and R4496C myocytes

Figure 6. SR Ca^{2+} load at various stimulation frequencies. (A) Representative examples of SR Ca^{2+} load assessed during rapid application of 20 mM caffeine and calculated from the integration of the inward NCX current at 1 Hz (top) and 3 Hz (bottom). (B) Mean ± SE data of SR Ca^{2+} content at 1-, 2-, and 3-Hz stimulation frequencies. SR Ca^{2+} content in R4496C ($n = 34$ and 5) myocytes is significantly below WT ($n = 27$ and 4) at all stimulation rates investigated. The difference is more pronounced at high rates (e.g., 3 Hz). *, P < 0.01 versus WT at all three frequencies; unpaired Student's t test.

(Fig. 5, A and B), and no differences were observed in the amplitude and voltage dependency of L-type Ca^{2+} current (Fig. 5, C and D).

Under the same basal conditions used in trabeculae (30°C, 2 mM $[Ca^{2+}]_o$), Ca^{2+}-transient amplitude and kinetics did not differ between R4496C and WT cardiomyocytes (Fig. 5, E and F) at a 1-Hz stimulation rate, in line with the absence of contractile impairment observed under basal conditions in intact R4496C trabeculae. However, when cardiomyocytes were paced at higher frequencies (2–3 Hz), Ca^{2+}-transient amplitude of R4496 cardiomyocytes was reduced with respect to WT (Fig. 5, E and F).

R4496C and WT myocytes were then rapidly exposed to 10 mM caffeine after a train of conditioning depolarizing steps at 1, 2, and 3 Hz, to study SR Ca^{2+} content, as calculated from the integral of NCX current (Fig. 6 A). SR Ca^{2+} content in R4496C myocytes was slightly reduced compared with WT at 1 Hz (-16%), in agreement with previous observations on the same transgenic model (Kashimura et al., 2010). The difference in SR Ca^{2+} content between R4496C and WT myocytes became larger at higher stimulation rates, reaching -34% at 3 Hz (Fig. 6 B). These results indicate that R4496C cardiomyocytes are able to maintain Ca^{2+}-transient amplitude despite a lower SR Ca^{2+} content at low inotropic levels, i.e., 1 Hz. However, the reduced ability to store Ca^{2+} in the SR causes a blunted Ca^{2+}-transient amplitude at higher pacing rates.

When stimulation pauses were introduced in a series of regularly paced Ca^{2+} transients at 3 Hz in current clamp, the post-rest increase of Ca^{2+}-transient amplitude was blunted in R4496C versus WT myocytes (Fig. 7, A and C), in agreement with the reduced post-rest potentiation of force observed in the mutant trabeculae. Interestingly, when SR Ca^{2+} content was measured by suddenly exposing the cell to caffeine after pauses of different durations, the physiological increase of SR Ca^{2+} content after the pause was absent in R4496C myocytes (Fig. 7, B and D). As an example, after a pause of 8 s, SR Ca^{2+} content increased by 21 ± 4% in WT, whereas it tended to decrease in R4496C cardiomyocytes (P < 0.05; Fig. 7 D). These results suggest that a reduced ability to accumulate Ca^{2+} in the SR during rest intervals underlies the blunted response to stimulation pauses. During stimulation pauses, diastolic intracellular Ca^{2+} oscillations (Fig. 7 A) were observed in 73% of R4496C ($n = 16/22$) versus 5% of WT ($n = 1/20$) myocytes (P < 0.01; Fisher's exact test). Consistently, spontaneous contractions were observed during long (60-s) rest intervals in 33% of R4496C trabeculae ($n = 4/12$) but were never seen in WT preparations ($n = 0/13$) (P < 0.01; Fisher's exact test). An increased rate of diastolic intracellular Ca^{2+} oscillations suggests enhanced spontaneous Ca^{2+} releases from the SR, which likely contribute to store depletion in R4496C myocytes and explain

the blunted increase in SR Ca^{2+} load during resting pauses (Fig. 7 D).

In agreement with previous findings (Liu et al., 2006; Fernández-Velasco et al., 2009; Kashimura et al., 2010), an increased occurrence of spontaneous diastolic intracellular $[Ca^{2+}]_i$ oscillations was also observed in R4496C versus WT ventricular cardiomyocytes under Iso (96% of R4496C myocytes vs. 38% of WT myocytes; P < 0.01; Fisher's exact test).

Mechanisms underlying the faster mechanical restitution of R4496C myocardium

Mechanical restitution of cardiac muscle reflects the interplay between sarcolemma and SR refractoriness. Specifically, for very premature beats, e.g., <100 ms, electrical refractoriness and I_{Ca-L} recovery are the major determinants of the mechanical phenomenon (Franz, 2003); recovery of calcium release (dictated by RyR gating properties; Banijamali et al., 1991; Kornyeyev et al., 2012; Brunello et al., 2013) and the rate of SR Ca^{2+} refilling (Poggesi et al., 1987) affect the later stages, when sarcolemma recovery is already completed. To understand the mechanisms underlying the faster mechanical restitution observed in R4496C intact myocardium, we evaluated the restitution rates of I_{Ca-L}, Ca^{2+} transient, and SR Ca^{2+} content in ventricular myocytes using specific patch-clamp protocols. All restitution curves display the fractional

recovery of the studied parameter plotted against the duration of the premature interval. As expected, the faster mechanical restitution (Fig. 8 A) was paralleled by a quicker recovery of Ca^{2+}-transient amplitude in R4496C ventricular myocytes (Fig. 8 B). No differences were present between R4496C and WT cardiomyocytes in terms of membrane electrical refractoriness (54 ± 6 ms in R4496C vs. 57 ± 7 ms in WT; P = 0.45) and the recovery properties of I_{Ca-L} (Fig. 8 A). Furthermore, we evaluated the rate of SR Ca^{2+} content recovery by rapidly exposing regularly stimulated cardiomyocytes to caffeine at different premature intervals (Fig. 8 C). SR Ca^{2+} recovery rate was similar in R4496C and WT cells (Fig. 8 D). This supports the hypothesis that R4496C mutation speeds up restitution by altering the gating properties of the RyR2 and not by increasing the rate of SR refilling.

Mathematical model

Experimental data from intact trabeculae and isolated cardiomyocytes were fitted into a validated cardiomyocyte computational model (Shannon et al., 2005; Garny et al., 2009; see supplemental file), where RyR2 gating is modulated by cytosolic $[Ca^{2+}]$ ($[Ca^{2+}]_i$) as well as by SR luminal $[Ca^{2+}]$ ($[Ca^{2+}]_{SR}$). To best simulate the features of the R4496C mutation, the rate constants of both activation and deactivation of RyR2 channels were modified, as detailed in the supplemental file. In line
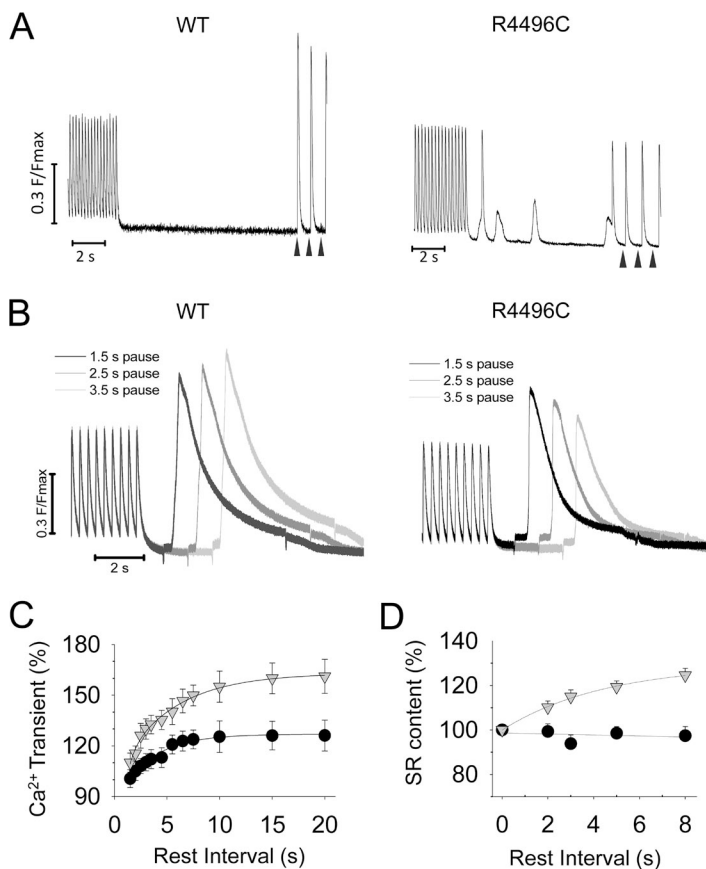
Figure 7. Effects of pauses on Ca^{2+} transients and SR Ca^{2+} load. (A) Representative traces of Ca^{2+} transients from R4496C and WT ventricular myocytes during stimulation pauses imposed after a conditioning stimulation at 3 Hz. Arrows mark the first beats triggered by external stimulation after the resting period. The amplitude of the first peak is analyzed to assess post-rest potentiation of Ca^{2+}-transient amplitude. Diastolic intracellular Ca^{2+} oscillations and spontaneous Ca^{2+} transients occur in the R4496C ventricular myocyte during the stimulation pause. (B) Simultaneous Ca^{2+} fluorescence traces recorded during the application of caffeine at different resting intervals, after a conditioning stimulation at 3 Hz in WT (left) and R4496C (right) myocytes. Traces where caffeine is delivered after pauses of different duration (1.5–3.5 s; conditioning activation train at 3 Hz) are shown superimposed. (C and D) Average percent increase of Ca^{2+}-transient amplitude (C) and SR Ca^{2+} load (D) after stimulation pauses of different duration in R4496C ($n = 22$ and 5) versus WT ($n = 20$ and 4) ventricular myocytes. Error bars represent mean ± SEM.

with the experimental results the model correctly predicts that at low inotropic levels (e.g., 1-Hz stimulation frequency, 2 mM $[Ca^{2+}]_{out}$), isometric twitch force and SR Ca^{2+} release are preserved in the mutant muscle despite a mild reduction of SR Ca^{2+} load (Fig. 9, top). Conversely, at higher inotropic levels (e.g., when stimulation frequency is raised up to 3 Hz), SR Ca^{2+} load is not able to properly increase in R4496C myocytes, resulting in reduced SR Ca^{2+} release and twitch amplitude (Fig. 9, bottom). The model supports the hypothesis that the contractile alterations observed in R4496C myocardium are a direct consequence of the altered RyR2 gating caused by the mutation. Based on model results, we conclude that R4496C mutation changes the kinetics of both activation and deactivation of mutant RyR2 channels, as suggested by previous studies on single mutant channels (Jiang et al., 2002, 2004).

DISCUSSION

The impact of CPVT-related RyR2 mutations on cardiac muscle contractility was investigated using a validated knock-in mouse model carrying the R4496C mutation (Cerrone et al., 2005; Liu et al., 2006; Fernández-Velasco et al., 2009). We compared heterozygous R4496C mice with WT siblings. Previous work on these mutant mice was focused on the pro-arrhythmogenic significance of the R4496C mutation, demonstrating enhanced diastolic SR Ca^{2+} leakage (Kashimura et al., 2010) and DADs at the cellular level (Liu et al., 2006), paralleled by ventricular and supraventricular arrhythmias in the whole heart (Cerrone et al., 2005, 2007). Here, we studied the R4496C mutation from the mechanical perspective, recording twitch tension from intact trabeculae in isometric, load-controlled conditions. We found that the R4496C mutation impairs contractility of both atrial and ventricular myocardium, consistently with ubiquitous RyR2 expression in the heart. Although steady-state systolic Ca^{2+} release and force development under basal experimental conditions are normal, upon inotropic stimulations, which resemble stress or exercise conditions (i.e., β-adrenergic activation or high beating rates), atrial and ventricular myocardium of R4496C mice show impaired ability to raise SR Ca^{2+} load, increase the
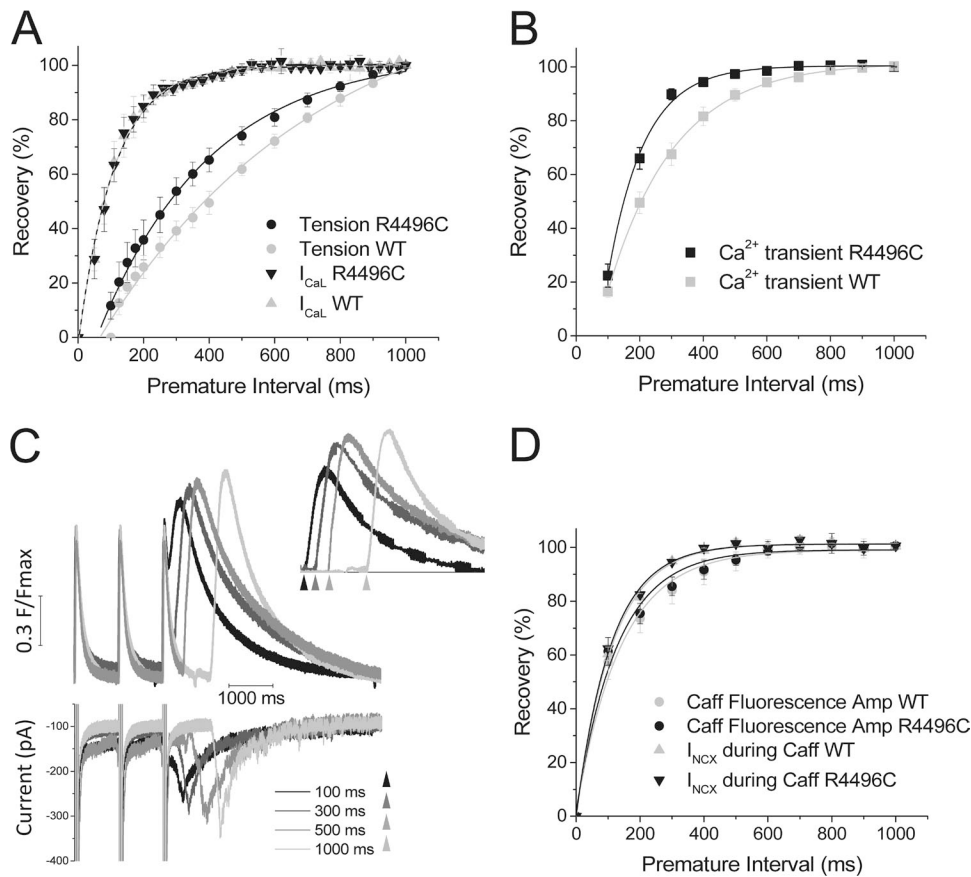
Figure 8. Restitution of twitches, L-type Ca^{2+} current, Ca^{2+} transients, and SR Ca^{2+} load in ventricular myocardium. All restitution curves are fitted by a single exponential to obtain restitution rates ($1/\tau$). (A) Average mechanical restitution curves from nine WT ($n = 7$) and nine R4496C ($n = 8$) ventricular trabeculae and L-type Ca^{2+} current recovery curves from 15 WT ($n = 3$) and 14 R4496C ($n = 3$) myocytes are shown superimposed. Rates for mechanical restitution: 1.96 ± 0.11 s^{-1} in WT and 2.63 ± 0.34 s^{-1} in R4496C; $P < 0.01$. Rates for L-type Ca^{2+} current recovery: 8.68 ± 0.35 s^{-1} in WT and 8.79 ± 0.41 s^{-1} in R4496C; $P = 0.51$. (B) Average curves showing the restitution of Ca^{2+}-transient amplitude in 21 WT ($n = 4$) and 23 R4496C ($n = 5$) ventricular myocytes. Rates: 3.72 ± 0.34 s^{-1} in WT and 5.33 ± 0.64 s^{-1} in R4496C; $P < 0.05$. (C) Representative examples of simultaneous intracellular Ca^{2+}-transient and membrane current recordings during rapid application of 20 mM caffeine at different premature intervals. (Inset) Caffeine-induced Ca^{2+} transient obtained by subtracting the average shape of the preceding regular Ca^{2+} transients from the fused traces. (D) SR Ca^{2+} load recovery curves calculated from both the amplitude of caffeine-induced Ca^{2+} transient and the integration of inward NCX current. Data are derived from 13 WT ($n = 3$) and 15 R4496C ($n = 3$) myocytes. Rates calculated from caffeine-induced Ca^{2+} transient: 7.15 ± 0.21 s^{-1} in WT and 7.71 ± 0.29 s^{-1} in R4496C; $P = 0.48$. Rates calculated from integration of the inward NCX current: 8.63 ± 0.23 s^{-1} in WT and 8.74 ± 0.31 s^{-1} in R4496C; $P = 0.48$. Error bars represent mean ± SEM.

amount of Ca^{2+} released from the SR, and enhance contractile force. Positive inotropic interventions, such as high $[Ca^{2+}]_{out}$ and long stimulation pauses, produced similar results. Consistently, we found enhanced occurrence of spontaneous Ca^{2+} oscillations during pauses and β-adrenergic stimulation in single cells, which suggests increased diastolic SR Ca^{2+} losses. Consistently, Fernández-Velasco et al. (2009) reported enhanced occurrence of Ca^{2+} sparks in unstimulated R4496C myocytes (resembling long stimulation pauses); Sedej et al. (2010) showed a larger increase in Ca^{2+} wave amplitude and frequency in R4496C myocytes by raising SR Ca^{2+} load with ouabain. Interestingly, the kinetics of Ca^{2+} transients and force twitches were always preserved in R4496C myocardium, both at baseline and under different inotropic challenges.
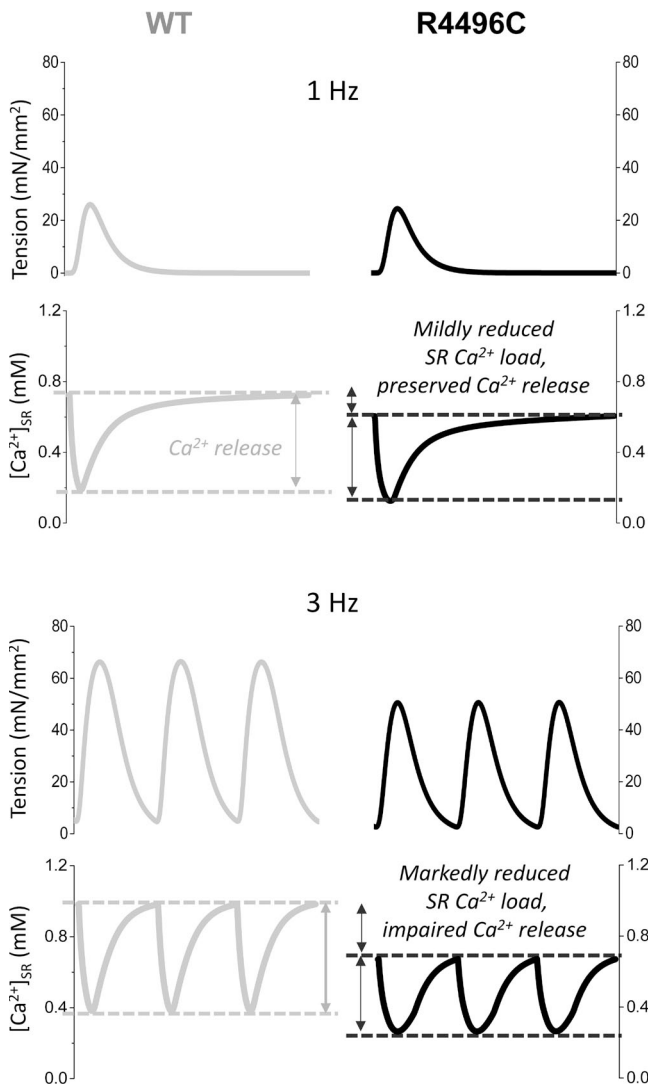
Figure 9. Cardiomyocyte computational model of R4496C RyR2 mutation. Simulations of twitch tension and SR Ca^{2+} changes at steady state during stimulation at different frequencies (1 and 3 Hz) in WT- and R4496C-modeled cells.

Of note, the intrinsic limitations of single cardiomyocyte studies prevented us from testing pacing frequencies higher than 3 Hz in cells. Intact trabeculae, however, were paced up to 7 Hz, which is well within the physiological range of mouse heart rates. At 7 Hz, mechanical impairment in R4496C atrial and ventricular trabeculae was larger than that seen at 3 Hz; therefore, we can predict that the underlying changes of Ca^{2+} transients and SR Ca^{2+} load would also be larger in the physiological range of frequencies (7–10 Hz).

Although the R4496C mutation is the initiating element, secondary changes, perhaps compensatory, may contribute to determining the observed SR Ca^{2+} load depletion and contractile alterations. The following arguments exclude a role of changes other than those introduced by the mutation itself. A relative reduction of SR Ca^{2+} ATPase (SERCA) versus NCX function could lead to reduced SR Ca^{2+} load. However, in R4496C, there is no increase in NCX activity as estimated from caffeine-induced Ca^{2+}-transient decay rate and no hints of reduced SERCA function (e.g., no slower Ca^{2+}-transient decay), phospholamban expression, or phosphorylation (Fernández-Velasco et al., 2009; Kashimura et al., 2010). Reduced sarcolemmal Ca^{2+} influx could impair Ca^{2+} accumulation in R4496C myocytes, but no difference between R4496C and WT myocytes was found in the amplitude, voltage dependence, and recovery of I_{Ca-L}. Ca^{2+}-transient and force decay rates are similarly accelerated by isoproterenol in R4496C and WT ventricular preparations. This rules out major alterations of the β-adrenergic receptor response in R4496C mice. Finally, previous work has shown that in R4496C myocardium, RyR2 expression and phosphorylation levels are unchanged (Fernández-Velasco et al., 2009).

We conclude that all contractile alterations observed in cardiac muscle from R4496C mice can be accounted for by changes in RyR2 channel gating. Single-channel recordings on HEK293 cells re-expressing RyR2 mutant channels have shown that the R4496C mutation increases RyR2 P_o by approximately three times by destabilizing the closed state of the channel; mean closed time was several times shorter in R4496C RyR2 compared with WT channel, whereas mean opening time was mildly affected (Jiang et al., 2002, 2004). Because of the increased sensitivity of mutant RyR2 activation to luminal $[Ca^{2+}]$, the threshold SR Ca^{2+} load at which spontaneous SR Ca^{2+} release and Ca^{2+} waves occur is lower in R4496C myocytes compared with WT; as a consequence, positive inotropic interventions are less effective at increasing SR Ca^{2+} load (Kashimura et al., 2010) caused by increased loss of SR Ca^{2+} during diastole. At baseline conditions, the increased SR fractional release caused by the altered channel gating of mutant RyR2 helps maintain Ca^{2+}-transient and twitch amplitudes despite a slightly reduced SR Ca^{2+} load (Jiang et al., 2002; Eisner et al., 2009). According to our results, under

inotropic challenge, the increased SR fractional release can no longer compensate for the reduced SR Ca^{2+} content in the mutant myocardium, ultimately resulting in contractile dysfunction. To better analyze this hypothesis, we fit the data into a computational cardiomyocyte model where RyR2 gating is represented by a four-state equilibrium modulated by SR Ca^{2+} concentration ($[Ca^{2+}]_{SR}$) (Iyer et al., 2007). The cardiomyocyte computational model used here helped us dissect the individual role of activating and deactivating RyR2 transitions in terms of their mechanical implications. Termination of Ca^{2+} release occurs when the local decrease of SR $[Ca^{2+}]$ triggers RyR2 deactivation via a specific luminal Ca^{2+} sensor located on the N terminus of the channel (Liu et al., 2015). Most CPVT-associated RyR2 mutations increase the sensitivity of activating RyR2 transition to SR $[Ca^{2+}]$ (Jiang et al., 2004); the same mutations may also alter the luminal Ca^{2+} dependency of RyR2 deactivation. In our mathematical model, to mimic the effects of R4496C mutation, RyR2 activation rates were increased and deactivation rates were decreased. When both activating and deactivating RyR2 transitions were modified, the model showed the full spectrum of changes that were experimentally observed in R4496C cells and trabeculae. When only the activation rates were modified, SR Ca^{2+} load was reduced and positive inotropic responses were blunted, in agreement with the experimental results obtained in R4496C preparations. However, in contrast with present experimental observations, Ca^{2+}-transient and twitch amplitudes were decreased even at basal conditions, whereas their kinetics were faster. Faster Ca^{2+}-transient kinetics as a consequence of the increase of RyR2 activation rates has been described previously in computational studies (Iyer et al., 2007). When only the RyR2-activating transitions are modified, there is no increase of SR fractional release at a low inotropic level, where a lower SR Ca^{2+} load leads to lower Ca^{2+} transients and force (Fig. S2). Changes in both activation and deactivation rates appear to be essential for the model to correctly predict the functional effects of the mutant RyR2, suggesting that R4496C mutation not only increases the P_o of the channel but also delays Ca^{2+} release termination (Fig. 9). In summary, R4496C mutation may not only increase the rate of channel activation in response to high luminal Ca^{2+} load during diastole but may also allow the RyR2 channel to release more Ca^{2+} during systole, by shifting the SR trigger for deactivation toward lower SR Ca^{2+} load. To validate this hypothesis, additional single-channel studies investigating the alterations of channel deactivation in the presence of CPVT mutations are warranted. Remarkably, changes of RyR2 gating are sufficient to predict both the impaired force–frequency response and the faster mechanical restitution in R4496C myocardium, supporting the idea that no secondary functional changes are involved in

determining mechanical abnormalities in CPVT. Other CPVT-associated RyR2 mutations have been shown to similarly affect channel gating (Jiang et al., 2004) and thus, hypothetically, myocardial contractile responses. Interestingly, reduced inotropic responses and faster mechanical restitution were also observed in a mouse model of CPVT carrying a point mutation in CASQ2: in this model, a mutation of the SR lumen protein calsequestrin determines shorter RyR2 refractoriness by causing an impairment of store-dependent RyR2 deactivation (Rizzi et al., 2008). It is still unclear whether the control of RyR2 gating by luminal Ca^{2+} is an intrinsic property of the channel (Chen et al., 2014; Liu et al., 2015) or depends on the interaction of Ca^{2+}-bound calsequestrin with RyR2 via the triadin–junctin complex (Györke and Terentyev, 2008; Ramay et al., 2011). However, observations from RyR2 (Liu et al., 2013) and CASQ2 mutants (Brunello et al., 2013) as well as animal models of ischemia (Belevych et al., 2007, 2011, 2012) suggest that any primary or acquired pathological modifications leading to shorter RyR2 refractoriness determine a similar mechanical phenotype, regardless of the underlying molecular mechanism.

Implications for human pathology

The failure of R4496C myocardium to increase force upon inotropic challenges contrasts with the apparent lack of functional impairment and/or cardiomyopathy in CPVT mutant mice and patients. Although intact trabeculae are a good approximation of the whole myocardium, the isometric conditions may somewhat enhance the difference between mutants and WT: a relatively large difference of peak twitch force in trabeculae could translate in a smaller decrease of cardiac output in the whole heart. Indeed, numerous hemodynamic adaptations may occur in vivo and ameliorate the effects of a reduced SR Ca^{2+} load reserve, thus avoiding development of overt cardiomyopathy. For example, in mice and patients with RyR2 mutations, resting bradycardia is commonly observed (Leenhardt et al., 1995; Priori et al., 2002; Neco et al., 2012). Lower heart rate may help maintain stroke volume via prolonged diastolic filling and increased end-diastolic volumes, despite mildly reduced contractility. Stress echocardiography on patients with R4497C RyR2 mutation could shed light on possible contractile impairment during exercise but, unfortunately, no such detailed assessments are available (Leenhardt et al., 1995). Indeed, as physical exertion and stress are the main triggers for arrhythmias in CPVT, diagnosed patients are instructed to forgo sport activity and symptom-limited ECG stress tests are performed only at the time of diagnosis and are avoided during clinical follow-up (Hayashi et al., 2009; van der Werf et al., 2012a; Wangüemert et al., 2015). Furthermore, the majority of CPVT patients are under β-blocker therapy, usually with potent, unselective agents such as

propranolol or nadolol (van der Werf et al., 2012b), or are subjected to cardiac left sympathetic denervation (De Ferrari et al., 2015): both strategies cause a marked limitation to the exercise capacity of patients. Therefore, it is hard to determine whether exercise limitation caused by contractile dysfunction is present in CPVT patients, and further investigation on selected patient cohorts is warranted.

The stress-induced contractile dysfunction caused by RyR2 mutations may contribute to the induction of arrhythmias during exercise in CPVT patients. The insufficient increase of cardiac output may create a positive feedback on the sympathetic system leading to hyperactivation of the adrenergic response. In addition, a marked contractile dysfunction leading to reduced cardiac output at high heart rates may cause myocardial perfusion deficit in the sub-endocardium, increasing the dispersion of repolarization, thereby promoting the degeneration of ventricular tachycardia to reentry-based ventricular fibrillation (Viitasalo et al., 2008).

A reduced contractile reserve, that scarcely affects contractile function of young patients, may significantly reduce tolerance to a sustained high mechanical load, e.g., in the presence of hypertension. Recent work on a RyR2 mutant mouse model showed that the mutation favors the development of cardiac hypertrophy and heart failure in response to chronic pressure overload (van Oort et al., 2010) or overexpression of CaMKIIδc (Dybkova et al., 2011). Because of its relatively poor prognosis, CPVT is usually diagnosed in adolescents and young adults; thus, all patient cohorts described in the literature are mainly comprised of young patients (Hayashi et al., 2009; Wangüemert et al., 2015). This makes it hard to predict how CPVT patients would respond to aging and aging-related cardiac illnesses, such as hypertension or coronary heart disease. This aspect may become clearer in the near future, as patient survival has significantly increased thanks to the use of implantable cardiac defibrillators and the introduction of new therapeutic strategies in addition to β blockers (e.g., flecainide, cardiac sympathetic denervation) (van der Werf et al., 2011; De Ferrari et al., 2015).

RyR2 mutations can directly cause arrhythmogenic right ventricular cardiomyopathy (Milting et al., 2006), where stress and exercise-induced arrhythmias are associated with a marked mechanical impairment of the right ventricle; the mechanisms shown here may explain the development of right-ventricular dysfunction and dilatation in RyR2-linked arrhythmogenic right ventricular cardiomyopathy.

Besides the rare disease-causing RyR2 mutations, a larger number of more common RyR2 polymorphisms may similarly affect RyR2 gating properties, although to a minor extent. These RyR2 polymorphisms, although benign in healthy patients, may modify the phenotypic expression of primary and secondary cardiomyopathies

by altering the mechanical properties of myocardium under stress.

Finally, increased phosphorylation of RyR2, either by PKA or by CaMKII, has been found in human and animal models of genetic cardiomyopathies (i.e., hypertrophic cardiomyopathy; Coppini et al., 2013) and acquired cardiac diseases (i.e., ischemic heart failure; Fischer et al., 2013), leading to changes of RyR2 gating that resemble CPVT-related mutations. In line with our results, we can speculate that changes of RyR2 gating caused by hyperphosphorylation may significantly contribute to contractile dysfunction in many acquired cardiac diseases. Pharmacological modulation of RyR2 gating in cardiac diseases may therefore be beneficial not only for arrhythmia reduction but also for contractile improvement.

REFERENCES

Ásgrímsson, H., M. Jóhannsson, and S.A. Arnardóttir. 1995. Excitation and contraction in atrial and ventricular myocardium of the guinea-pig. *Acta Physiol. Scand.* 153:133–141. http://dx.doi.org/10.1111/j.1748-1716.1995.tb09844.x

Banijamali, H.S., W.D. Gao, B.R. MacIntosh, and H.E. ter Keurs. 1991. Force-interval relations of twitches and cold contractures in rat cardiac trabeculae. Effect of ryanodine. *Circ. Res.* 69:937–948. http://dx.doi.org/10.1161/01.RES.69.4.937

Belevych, A., Z. Kubalova, D. Terentyev, R.L. Hamlin, C.A. Carnes, and S. Györke. 2007. Enhanced ryanodine receptor-mediated calcium leak determines reduced sarcoplasmic reticulum calcium content in chronic canine heart failure. *Biophys. J.* 93:4083–4092. http://dx.doi.org/10.1529/biophysj.107.114546

Belevych, A.E., D. Terentyev, R. Terentyeva, Y. Nishijima, A. Sridhar, R.L. Hamlin, C.A. Carnes, and S. Györke. 2011. The relationship between arrhythmogenesis and impaired contractility in heart failure: role of altered ryanodine receptor function. *Cardiovasc. Res.* 90:493–502. http://dx.doi.org/10.1093/cvr/cvr025

Belevych, A.E., D. Terentyev, R. Terentyeva, H.T. Ho, I. Gyorke, I.M. Bonilla, C.A. Carnes, G.E. Billman, and S. Györke. 2012. Shortened Ca^{2+} signaling refractoriness underlies cellular arrhythmogenesis in a postinfarction model of sudden cardiac death. *Circ. Res.* 110:569–577. http://dx.doi.org/10.1161/CIRCRESAHA.111.260455

Bers, D.M. 2002. Cardiac excitation-contraction coupling. *Nature.* 415:198–205. http://dx.doi.org/10.1038/415198a

Bers, D.M., and M. Fill. 1998. Coordinated feet and the dance of ryanodine receptors. *Science.* 281:790–791. http://dx.doi.org/10.1126/science.281.5378.790

Bondarenko, V.E., G.P. Szigeti, G.C. Bett, S.J. Kim, and R.L. Rasmusson. 2004. Computer model of action potential of mouse ventricular myocytes. *Am. J. Physiol. Heart Circ. Physiol.* 287:H1378–H1403. http://dx.doi.org/10.1152/ajpheart.00185.2003

Brunello, L., J.L. Slabaugh, P.B. Radwanski, H.T. Ho, A.E. Belevych, Q. Lou, H. Chen, C. Napolitano, F. Lodola, S.G. Priori, et al. 2013. Decreased RyR2 refractoriness determines myocardial

synchronization of aberrant Ca^{2+} release in a genetic model of arrhythmia. *Proc. Natl. Acad. Sci. USA.* 110:10312–10317. http://dx.doi.org/10.1073/pnas.1300052110

Cerrone, M., B. Colombi, M. Santoro, M.R. di Barletta, M. Scelsi, L. Villani, C. Napolitano, and S.G. Priori. 2005. Bidirectional ventricular tachycardia and fibrillation elicited in a knock-in mouse model carrier of a mutation in the cardiac ryanodine receptor. *Circ. Res.* 96:e77–e82. http://dx.doi.org/10.1161/01.RES.0000169067.51055.72

Cerrone, M., S.F. Noujaim, E.G. Tolkacheva, A. Talkachou, R. O'Connell, O. Berenfeld, J. Anumonwo, S.V. Pandit, K. Vikstrom, C. Napolitano, et al. 2007. Arrhythmogenic mechanisms in a mouse model of catecholaminergic polymorphic ventricular tachycardia. *Circ. Res.* 101:1039–1048. http://dx.doi.org/10.1161/CIRCRESAHA.107.148064

Chen, B., A. Guo, Z. Gao, S. Wei, Y.P. Xie, S.R. Chen, M.E. Anderson, and L.S. Song. 2012. In situ confocal imaging in intact heart reveals stress-induced Ca^{2+} release variability in a murine catecholaminergic polymorphic ventricular tachycardia model of type 2 ryanodine receptor$^{R4496C+/-}$ mutation. *Circ Arrhythm Electrophysiol.* 5:841–849. http://dx.doi.org/10.1161/CIRCEP.111.969733

Chen, W., R. Wang, B. Chen, X. Zhong, H. Kong, Y. Bai, Q. Zhou, C. Xie, J. Zhang, A. Guo, et al. 2014. The ryanodine receptor store-sensing gate controls Ca^{2+} waves and Ca^{2+}-triggered arrhythmias. *Nat. Med.* 20:184–192. http://dx.doi.org/10.1038/nm.3440

Cooper, I.C., and C.H. Fry. 1990. Mechanical restitution in isolated mammalian myocardium: Species differences and underlying mechanisms. *J. Mol. Cell. Cardiol.* 22:439–452. http://dx.doi.org/10.1016/0022-2828(90)91479-Q

Coppini, R., C. Ferrantini, L. Yao, P. Fan, M. Del Lungo, F. Stillitano, L. Sartiani, B. Tosi, S. Suffredini, C. Tesi, et al. 2013. Late sodium current inhibition reverses electromechanical dysfunction in human hypertrophic cardiomyopathy. *Circulation.* 127:575–584. http://dx.doi.org/10.1161/CIRCULATIONAHA.112.134932

De Ferrari, G.M., V. Dusi, C. Spazzolini, J.M. Bos, D.J. Abrams, C.I. Berul, L. Crotti, A.M. Davis, M. Eldar, M. Kharlap, et al. 2015. Clinical management of catecholaminergic polymorphic ventricular tachycardia: The role of left cardiac sympathetic denervation. *Circulation.* 131:2185–2193. http://dx.doi.org/10.1161/CIRCULATIONAHA.115.015731

Dybkova, N., S. Sedej, C. Napolitano, S. Neef, A.G. Rokita, M. Hünlich, J.H. Brown, J. Kockskämper, S.G. Priori, B. Pieske, and L.S. Maier. 2011. Overexpression of CaMKIIδc in RyR2$^{R4496C+/-}$ knock-in mice leads to altered intracellular Ca^{2+} handling and increased mortality. *J. Am. Coll. Cardiol.* 57:469–479. http://dx.doi.org/10.1016/j.jacc.2010.08.639

Eisner, D.A., T. Kashimura, S.C. O'Neill, L.A. Venetucci, and A.W. Trafford. 2009. What role does modulation of the ryanodine receptor play in cardiac inotropy and arrhythmogenesis? *J. Mol. Cell. Cardiol.* 46:474–481. http://dx.doi.org/10.1016/j.yjmcc.2008.12.005

Fernández-Velasco, M., A. Rueda, N. Rizzi, J.P. Benitah, B. Colombi, C. Napolitano, S.G. Priori, S. Richard, and A.M. Gómez. 2009. Increased Ca^{2+} sensitivity of the ryanodine receptor mutant RyR2^{R4496C} underlies catecholaminergic polymorphic ventricular tachycardia. *Circ. Res.* 104:201–209. http://dx.doi.org/10.1161/CIRCRESAHA.108.177493

Ferrantini, C., R. Coppini, L. Sacconi, B. Tosi, M.L. Zhang, G.L. Wang, E. de Vries, E. Hoppenbrouwers, F. Pavone, E. Cerbai, et al. 2014. Impact of detubulation on force and kinetics of cardiac muscle contraction. *J. Gen. Physiol.* 143:783–797. http://dx.doi.org/10.1085/jgp.201311125

Fischer, T.H., J. Herting, T. Tirilomis, A. Renner, S. Neef, K. Toischer, D. Ellenberger, A. Förster, J.D. Schmitto, J. Gummert, et al. 2013. Ca^{2+}/calmodulin-dependent protein kinase II and protein kinase A differentially regulate sarcoplasmic reticulum Ca^{2+} leak in human cardiac pathology. *Circulation.* 128:970–981. http://dx.doi.org/10.1161/CIRCULATIONAHA.113.001746

Franz, M.R. 2003. The electrical restitution curve revisited: Steep or flat slope—which is better? *J. Cardiovasc. Electrophysiol.* 14:S140–S147. http://dx.doi.org/10.1046/j.1540.8167.90303.x

Franzini-Armstrong, C., and F. Protasi. 1997. Ryanodine receptors of striated muscles: a complex channel capable of multiple interactions. *Physiol. Rev.* 77:699–729.

Garny, A., D. Noble, P.J. Hunter, and P. Kohl. 2009. CELLULAR OPEN RESOURCE (COR): current status and future directions. *Philos. Trans. A Math. Phys. Eng. Sci.* 367:1885–1905. http://dx.doi.org/10.1098/rsta.2008.0289

George, C.H., H. Jundi, N.L. Thomas, D.L. Fry, and F.A. Lai. 2007. Ryanodine receptors and ventricular arrhythmias: Emerging trends in mutations, mechanisms and therapies. *J. Mol. Cell. Cardiol.* 42:34–50. http://dx.doi.org/10.1016/j.yjmcc.2006.08.115

Györke, S., and D. Terentyev. 2008. Modulation of ryanodine receptor by luminal calcium and accessory proteins in health and cardiac disease. *Cardiovasc. Res.* 77:245–255. http://dx.doi.org/10.1093/cvr/cvm038

Hayashi, M., I. Denjoy, F. Extramiana, A. Maltret, N.R. Buisson, J.M. Lupoglazoff, D. Klug, M. Hayashi, S. Takatsuki, E. Villain, et al. 2009. Incidence and risk factors of arrhythmic events in catecholaminergic polymorphic ventricular tachycardia. *Circulation.* 119:2426–2434. http://dx.doi.org/10.1161/CIRCULATIONAHA.108.829267

Iyer, V., R.J. Hajjar, and A.A. Armoundas. 2007. Mechanisms of abnormal calcium homeostasis in mutations responsible for catecholaminergic polymorphic ventricular tachycardia. *Circ. Res.* 100:e22–e31. http://dx.doi.org/10.1161/01.RES.0000258468.31815.42

Jiang, D., B. Xiao, L. Zhang, and S.R. Chen. 2002. Enhanced basal activity of a cardiac Ca^{2+} release channel (ryanodine receptor) mutant associated with ventricular tachycardia and sudden death. *Circ. Res.* 91:218–225. http://dx.doi.org/10.1161/01.RES.0000028455.36940.5E

Jiang, D., B. Xiao, D. Yang, R. Wang, P. Choi, L. Zhang, H. Cheng, and S.R. Chen. 2004. RyR2 mutations linked to ventricular tachycardia and sudden death reduce the threshold for store-overload-induced Ca^{2+} release (SOICR). *Proc. Natl. Acad. Sci. USA.* 101:13062–13067. http://dx.doi.org/10.1073/pnas.0402388101

Kannankeril, P.J., B.M. Mitchell, S.A. Goonasekera, M.G. Chelu, W. Zhang, S. Sood, D.L. Kearney, C.I. Danila, M. De Biasi, X.H. Wehrens, et al. 2006. Mice with the R176Q cardiac ryanodine receptor mutation exhibit catecholamine-induced ventricular tachycardia and cardiomyopathy. *Proc. Natl. Acad. Sci. USA.* 103:12179–12184. http://dx.doi.org/10.1073/pnas.0600268103

Kashimura, T., S.J. Briston, A.W. Trafford, C. Napolitano, S.G. Priori, D.A. Eisner, and L.A. Venetucci. 2010. In the RyR2^{R4496C} mouse model of CPVT, β-adrenergic stimulation induces Ca waves by increasing SR Ca content and not by decreasing the threshold for Ca waves. *Circ. Res.* 107:1483–1489. http://dx.doi.org/10.1161/CIRCRESAHA.110.227744

Korajoki, H., and M. Vornanen. 2012. Expression of SERCA and phospholamban in rainbow trout (*Oncorhynchus mykiss*) heart: comparison of atrial and ventricular tissue and effects of thermal acclimation. *J. Exp. Biol.* 215:1162–1169. http://dx.doi.org/10.1242/jeb.065102

Kornyeyev, D., A.D. Petrosky, B. Zepeda, M. Ferreiro, B. Knollmann, and A.L. Escobar. 2012. Calsequestrin 2 deletion shortens the refractoriness of Ca^{2+} release and reduces rate-dependent Ca^{2+}-alternans in intact mouse hearts. *J. Mol. Cell. Cardiol.* 52:21–31. http://dx.doi.org/10.1016/j.yjmcc.2011.09.020

Laitinen, P.J., K.M. Brown, K. Piippo, H. Swan, J.M. Devaney, B. Brahmbhatt, E.A. Donarum, M. Marino, N. Tiso, M. Viitasalo, et al.

2001. Mutations of the cardiac ryanodine receptor (RyR2) gene in familial polymorphic ventricular tachycardia. *Circulation*. 103:485–490. http://dx.doi.org/10.1161/01.CIR.103.4.485

Lanner, J.T., D.K. Georgiou, A.D. Joshi, and S.L. Hamilton. 2010. Ryanodine receptors: Structure, expression, molecular details, and function in calcium release. *Cold Spring Harb. Perspect. Biol.* 2:a003996. http://dx.doi.org/10.1101/cshperspect.a003996

Leenhardt, A., V. Lucet, I. Denjoy, F. Grau, D.D. Ngoc, and P. Coumel. 1995. Catecholaminergic polymorphic ventricular tachycardia in children. A 7-year follow-up of 21 patients. *Circulation*. 91:1512–1519. http://dx.doi.org/10.1161/01.CIR.91.5.1512

Liu, N., B. Colombi, M. Memmi, S. Zissimopoulos, N. Rizzi, S. Negri, M. Imbriani, C. Napolitano, F.A. Lai, and S.G. Priori. 2006. Arrhythmogenesis in catecholaminergic polymorphic ventricular tachycardia: Insights from a RyR2 R4496C knock-in mouse model. *Circ. Res.* 99:292–298. http://dx.doi.org/10.1161/01.RES.0000235869.50747.e1

Liu, Y., L. Kimlicka, F. Hiess, X. Tian, R. Wang, L. Zhang, P.P. Jones, F. Van Petegem, and S.R. Chen. 2013. The CPVT-associated RyR2 mutation G230C enhances store overload-induced Ca^{2+} release and destabilizes the N-terminal domains. *Biochem. J.* 454:123–131. http://dx.doi.org/10.1042/BJ20130594

Liu, Y., B. Sun, Z. Xiao, R. Wang, W. Guo, J.Z. Zhang, T. Mi, Y. Wang, P.P. Jones, F. Van Petegem, and S.R. Chen. 2015. Roles of the NH_2-terminal domains of cardiac ryanodine receptor in Ca^{2+} release activation and termination. *J. Biol. Chem.* 290:7736–7746. http://dx.doi.org/10.1074/jbc.M114.618827

Milting, H., N. Lukas, B. Klauke, R. Körfer, A. Perrot, K.J. Osterziel, J. Vogt, S. Peters, R. Thieleczek, and M. Varsányi. 2006. Composite polymorphisms in the ryanodine receptor 2 gene associated with arrhythmogenic right ventricular cardiomyopathy. *Cardiovasc. Res.* 71:496–505. http://dx.doi.org/10.1016/j.cardiores.2006.04.004

Mohamed, U., C. Napolitano, and S.G. Priori. 2007. Molecular and electrophysiological bases of catecholaminergic polymorphic ventricular tachycardia. *J. Cardiovasc. Electrophysiol.* 18:791–797. http://dx.doi.org/10.1111/j.1540-8167.2007.00766.x

Neco, P., A.G. Torrente, P. Mesirca, E. Zorio, N. Liu, S.G. Priori, C. Napolitano, S. Richard, J.P. Benitah, M.E. Mangoni, and A.M. Gómez. 2012. Paradoxical effect of increased diastolic Ca^{2+} release and decreased sinoatrial node activity in a mouse model of catecholaminergic polymorphic ventricular tachycardia. *Circulation*. 126:392–401. http://dx.doi.org/10.1161/CIRCULATIONAHA.111.075382

Poggesi, C., M. Everts, B. Polla, F. Tanzi, and C. Reggiani. 1987. Influence of thyroid state on mechanical restitution of rat myocardium. *Circ. Res.* 60:142–151. http://dx.doi.org/10.1161/01.RES.60.1.142

Priori, S.G., C. Napolitano, M. Memmi, B. Colombi, F. Drago, M. Gasparini, L. DeSimone, F. Coltorti, R. Bloise, R. Keegan, et al. 2002. Clinical and molecular characterization of patients with catecholaminergic polymorphic ventricular tachycardia. *Circulation*. 106:69–74. http://dx.doi.org/10.1161/01.CIR.0000020013.73106.D8

Ramay, H.R., O.Z. Liu, and E.A. Sobie. 2011. Recovery of cardiac calcium release is controlled by sarcoplasmic reticulum refilling and ryanodine receptor sensitivity. *Cardiovasc. Res.* 91:598–605. http://dx.doi.org/10.1093/cvr/cvr143

Rice, J.J., R.L. Winslow, and W.C. Hunter. 1999. Comparison of putative cooperative mechanisms in cardiac muscle: length dependence and dynamic responses. *Am. J. Physiol.* 276:H1734–H1754.

Rizzi, N., N. Liu, C. Napolitano, A. Nori, F. Turcato, B. Colombi, S. Bicciato, D. Arcelli, A. Spedito, M. Scelsi, et al. 2008. Unexpected structural and functional consequences of the R33Q homozygous mutation in cardiac calsequestrin: A complex arrhythmogenic cascade in a knock in mouse model. *Circ. Res.* 103:298–306. http://dx.doi.org/10.1161/CIRCRESAHA.108.171660

Sedej, S., F.R. Heinzel, S. Walther, N. Dybkova, P. Wakula, J. Groborz, P. Gronau, L.S. Maier, M.A. Vos, F.A. Lai, et al. 2010. Na^+-dependent SR Ca^{2+} overload induces arrhythmogenic events in mouse cardiomyocytes with a human CPVT mutation. *Cardiovasc. Res.* 87:50–59. http://dx.doi.org/10.1093/cvr/cvq007

Shannon, T.R., F. Wang, J. Puglisi, C. Weber, and D.M. Bers. 2004. A mathematical treatment of integrated Ca dynamics within the ventricular myocyte. *Biophys. J.* 87:3351–3371. http://dx.doi.org/10.1529/biophysj.104.047449

Shannon, T.R., F. Wang, and D.M. Bers. 2005. Regulation of cardiac sarcoplasmic reticulum Ca release by luminal [Ca] and altered gating assessed with a mathematical model. *Biophys. J.* 89:4096–4110. http://dx.doi.org/10.1529/biophysj.105.068734

Shioya, T. 2007. A simple technique for isolating healthy heart cells from mouse models. *J. Physiol. Sci.* 57:327–335. http://dx.doi.org/10.2170/physiolsci.RP010107

Stull, L.B., M.K. Leppo, E. Marbán, and P.M. Janssen. 2002. Physiological determinants of contractile force generation and calcium handling in mouse myocardium. *J. Mol. Cell. Cardiol.* 34:1367–1376. http://dx.doi.org/10.1006/jmcc.2002.2065

Stuyvers, B.D., A.D. McCulloch, J. Guo, H.J. Duff, and H.E. ter Keurs. 2002. Effect of stimulation rate, sarcomere length and Ca^{2+} on force generation by mouse cardiac muscle. *J. Physiol.* 544:817–830. http://dx.doi.org/10.1113/jphysiol.2002.024430

van der Werf, C., P.J. Kannankeril, F. Sacher, A.D. Krahn, S. Viskin, A. Leenhardt, W. Shimizu, N. Sumitomo, F.A. Fish, Z.A. Bhuiyan, et al. 2011. Flecainide therapy reduces exercise-induced ventricular arrhythmias in patients with catecholaminergic polymorphic ventricular tachycardia. *J. Am. Coll. Cardiol.* 57:2244–2254. http://dx.doi.org/10.1016/j.jacc.2011.01.026

van der Werf, C., I. Nederend, N. Hofman, N. van Geloven, C. Ebink, I.M. Frohn-Mulder, A.M. Alings, H.A. Bosker, F.A. Bracke, F. van den Heuvel, et al. 2012a. Familial evaluation in catecholaminergic polymorphic ventricular tachycardia: Disease penetrance and expression in cardiac ryanodine receptor mutation-carrying relatives. *Circ Arrhythm Electrophysiol*. 5:748–756. http://dx.doi.org/10.1161/CIRCEP.112.970517

van der Werf, C., A.H. Zwinderman, and A.A. Wilde. 2012b. Therapeutic approach for patients with catecholaminergic polymorphic ventricular tachycardia: state of the art and future developments. *Europace*. 14:175–183. http://dx.doi.org/10.1093/europace/eur277

van Oort, R.J., J.L. Respress, N. Li, C. Reynolds, A.C. De Almeida, D.G. Skapura, L.J. De Windt, and X.H. Wehrens. 2010. Accelerated development of pressure overload-induced cardiac hypertrophy and dysfunction in an RyR2-R176Q knockin mouse model. *Hypertension*. 55:932–938. http://dx.doi.org/10.1161/HYPERTENSIONAHA.109.146449

Viitasalo, M., L. Oikarinen, H. Väänänen, K. Kontula, L. Toivonen, and H. Swan. 2008. U-waves and T-wave peak to T-wave end intervals in patients with catecholaminergic polymorphic ventricular tachycardia, effects of beta-blockers. *Heart Rhythm*. 5:1382–1388. http://dx.doi.org/10.1016/j.hrthm.2008.06.011

Wangüemert, F., C. Bosch Calero, C. Pérez, O. Campuzano, P. Beltran-Alvarez, F.S. Scornik, A. Iglesias, P. Berne, C. Allegue, P.M. Ruiz Hernandez, et al. 2015. Clinical and molecular characterization of a cardiac ryanodine receptor founder mutation causing catecholaminergic polymorphic ventricular tachycardia. *Heart Rhythm*. 12:1636–1643. http://dx.doi.org/10.1016/j.hrthm.2015.03.033